

# Fault-Tolerant Control with Active Fault Diagnosis for Four-Wheel Independently-Driven Electric Ground Vehicles

Rongrong Wang and Junmin Wang\*

**Abstract**—A fault-tolerant (FT) control approach for four-wheel independently-driven (4WID) electric vehicles is presented. An adaptive control based passive fault-tolerant controller is designed to ensure the system stability when an in-wheel motor/motor driver fault happens. As an over-actuated system, it is challenging to isolate the faulty wheel and accurately estimate the control gain of the faulty in-wheel motor for 4WID electric vehicles. An active fault diagnosis approach is thus proposed to isolate and evaluate the fault. Based on the estimated control gain of the faulty in-wheel motor, the control efforts of all the four wheels are redistributed to relieve the torque demand on the faulty wheel. Simulations using a high-fidelity, CarSim, full-vehicle model show the effectiveness of the proposed in-wheel motor/motor driver fault diagnosis and fault-tolerant control approach.

## I. INTRODUCTION

FOUR-wheel independently-driven (4WID) electric vehicle is an promising vehicle architecture due to its potentials in emissions and fuel consumption reductions [1]. A 4WID electric vehicle employs four in-wheel (or hub) motors to drive the four wheels, and the torque and driving/braking mode of each wheel can be controlled independently. Such actuation flexibility together with the electric motors' fast and precise torque responses can enhance the existing vehicle control strategies, e.g. traction control system (TCS) and direct yaw-moment control (DYC), and other advanced vehicle motion / stability control systems [2][3][23].

However, due to the significantly increased system complexity and number of actuators, the probability for a fault, e.g. in-wheel motor/motor driver fault, taking place in a 4WID electric vehicle is higher. The in-wheel motor faults may be caused by mechanical failures, overheat of the motors, or faults associated with the motor drivers. When such a fault occurs, the faulty wheel may fail to provide the expected torque and thus jeopardize the vehicle motion control. Without appropriate accommodations, the in-wheel motor or motor driver faults may result in vehicle performance deterioration or even instability due to loss of desired torque on a particular wheel [4][6]. Therefore, the demands on reliability, safety, and fault tolerance for 4WID electric vehicles are substantially elevated.

Several fault diagnosis and fault-tolerant (FT) control strategies for ground vehicles have been suggested in the

literatures [7][8][9][10][11]. However, most of these algorithms dealt with the problems associated with conventional vehicle architectures, but not for the 4WID electric vehicles. It is known that the 4WID electric vehicle is a typical over-actuated system, and the fault diagnosis design for such systems is challenging [12]. Yang proposed a FT path-tracking control for a 4WID electric vehicle [13][14], but the fault diagnosis approach was not presented. Fault diagnosis and FT control methods for electric motors are also proposed and reviewed in [15][17]. Some motor faults, such as the bearing faults, are difficult to diagnose with only current and voltage sensors [17]. Thus, these motor/motor controller diagnosis approaches are not used in this study.

This paper considers the vehicle dynamics-based fault diagnosis and FT control for 4WID electric vehicles. As an over-actuated system, the conventional fault diagnosis and FT control methods may not work for the 4WID electric vehicles. For example, the front and rear wheels on the same side of a vehicle have the same effect on the vehicle yaw and longitudinal motion dynamics when the vehicle is running in a straight line. Such features associated with the actuation redundancy make some of the FT controllers, such as the multiple model based approaches [19], difficult to be implemented on 4WID electric vehicles. An adaptive control based passive FT controller is designed to maintain the vehicle stability and desired motion when an in-wheel motor/motor driver fault happens. Then, an active fault diagnosis approach is proposed to isolate and evaluate the fault under the designed passive FT controller. Finally, the control efforts of all the in-wheel motors are readjusted based on the diagnosis result to relieve the torque demand on the faulty motor/motor driver for avoiding further damages. Simulations using a high-fidelity vehicle model illustrate the effectiveness of the proposed strategy.

The rest of the paper is organized as follows. System modeling is presented in section 2. The proposed FT controller is described in section 3. The active diagnosis method with control effort redistribution is proposed in section 4. Simulation results are presented in section 5 followed by conclusive remarks.

## II. SYSTEM MODELING AND PROBLEM FORMULATION

### A. Vehicle modeling

Ignoring the pitch and roll motion, the vehicle has three degrees of freedom for longitudinal motion, lateral motion and yaw motion. A schematic diagram of a vehicle model is shown in Figure 1.

\*Corresponding author. Rongrong Wang and Junmin Wang are with the Department of Mechanical and Aerospace Engineering, The Ohio State University, Columbus, OH 43210 USA (e-mail: wang.1862@buckeyemail.osu.edu; wang.1381@osu.edu). This research was supported by the Office of Naval Research Young Investigator Award under Grant N00014-09-1-1018, Honda-OSU Partnership Program, and OSU Transportation Research Endowment Program.

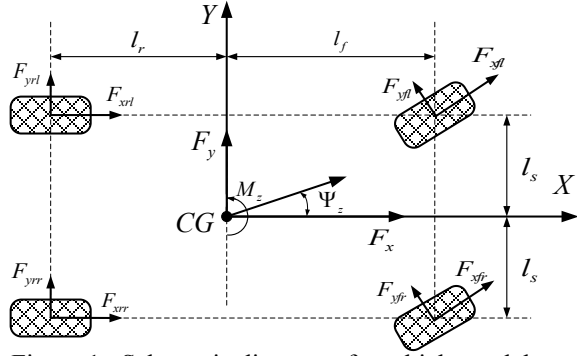


Figure 1. Schematic diagram of a vehicle model.

Vehicle equations of motion can be expressed as:

$$\begin{cases} \dot{V}_x = V_y \Omega_z - \frac{C_a}{M} V_x^2 + \frac{1}{M} F_x \\ \dot{V}_y = -V_x \Omega_z + \frac{1}{M} F_y \\ \dot{\Omega}_z = \frac{1}{I_z} M_z \end{cases}, \quad (1)$$

where  $V_x$  and  $V_y$  are longitudinal speed and lateral speed, respectively,  $\Omega_z$  is the yaw rate,  $M$  is the mass of the vehicle,  $I_z$  is the yaw inertia, and  $C_a$  is the aerodynamic drag term.  $F_x$ ,  $F_y$ , and  $M_z$  are the total forces/moment by the tire forces generated at all the four wheels, and can be defined by

$$\begin{cases} F_x = (F_{xfl} + F_{xfr}) \cos \sigma - (F_{yfl} + F_{yfr}) \sin \sigma + F_{xrl} + F_{xrr} \\ F_y = (F_{yfl} + F_{yfr}) \cos \sigma + (F_{xfl} + F_{xfr}) \sin \sigma + F_{yrl} + F_{yrr} \\ M_z = (F_{yfl} \sin \sigma - F_{xfl} \cos \sigma - F_{xrl} + F_{xrr} + F_{xfr} \cos \sigma \\ - F_{yfr} \sin \sigma) l_s - (F_{yfr} + F_{yrr}) l_r \\ + ((F_{yfr} + F_{xfl}) \cos \sigma + (F_{xfr} + F_{xfl}) \sin \sigma) l_f \end{cases} \quad (2)$$

where,  $\sigma$  is the front wheel steering angle. Based on (2), (1) can be rewritten as

$$\begin{bmatrix} \dot{V}_x \\ \dot{V}_y \\ \dot{\Omega}_z \end{bmatrix} = \begin{bmatrix} V_y \Omega_z - \frac{C_a}{M} V_x^2 \\ -V_x \Omega_z \\ 0 \end{bmatrix} + B_y F_y + B_x F_x, \quad (3)$$

where  $F_x = [F_{xfl} \ F_{xfr} \ F_{xrl} \ F_{xrr}]^T$ ,  $F_y = [F_{yfl} \ F_{yfr} \ F_{yrl} \ F_{yrr}]^T$  are the tire longitudinal and lateral forces, which can be calculated by a tire model based on measured tire slip ratios, slip angles, and normal loads. In this paper, the Magic Formula tire model [16] is used to calculate the tire forces. And a load transfer model can be used to calculate the tire normal load. The corresponding matrices are.

$$B_x = Q \begin{bmatrix} \cos \sigma & \cos \sigma & 1 & 1 \\ \sin \sigma & \sin \sigma & 0 & 0 \\ l_f \sin \sigma - l_s \cos \sigma & l_f \sin \sigma + l_s \cos \sigma & -l_s & l_s \end{bmatrix},$$

$$B_y = Q \begin{bmatrix} -\sin \sigma & -\sin \sigma & 0 & 0 \\ \cos \sigma & \cos \sigma & 1 & 1 \\ l_f \cos \sigma + l_s \sin \sigma & l_f \cos \sigma - l_s \sin \sigma & -l_r & -l_r \end{bmatrix},$$

with  $Q = \text{diag} \left[ \frac{1}{M} \ \frac{1}{M} \ \frac{1}{I_z} \right]$ .

The mechanical motion of a motor or a vehicle is much slower than a motor's electromagnetic dynamics, implying that the dynamics of the motor driver and in-wheel motor can be ignored. If each pair of in-wheel motor and driver is treated as a unit, the motor driver and motor pair model can be described by a control gain  $k_i$ , which is defined as

$$k_i = \frac{T_i}{u_i}, \quad (4)$$

where  $i \in S := \{fl \ fr \ rl \ rr\}$  indicates the specific wheel,  $T_i$

is the output torque of the in-wheel motor,  $u_i$  is the torque control signal to the motor's driver. Note that the control gain  $k_i$  can be obtained with experimental data. In general, if a fault happens to a certain motor and/or the motor driver, the corresponding control gain will be reduced.

The rotational dynamics of each wheel is represented by

$$I \dot{\omega}_i = k_i u_i - R_{eff} F_{xi}, \quad (5)$$

where  $\omega_i$  is the wheel longitudinal rotational speed in rad/s,  $R_{eff}$  is the tire effective rolling radius in meter, and  $I$  is the wheel moment of inertia. Thus, the above equation can be written as

$$F_{xi} = \frac{k_i u_i - I \dot{\omega}_i}{R_{eff}}. \quad (6)$$

So one can have

$$F_x = \frac{1}{R_{eff}} \begin{bmatrix} k_{fl} & 0 & 0 & 0 \\ 0 & k_{fr} & 0 & 0 \\ 0 & 0 & k_{rl} & 0 \\ 0 & 0 & 0 & k_{rr} \end{bmatrix} \begin{bmatrix} u_{fl} \\ u_{fr} \\ u_{rl} \\ u_{rr} \end{bmatrix} - \frac{1}{R_{eff}} \begin{bmatrix} I \dot{\omega}_{fl} \\ I \dot{\omega}_{fr} \\ I \dot{\omega}_{rl} \\ I \dot{\omega}_{rr} \end{bmatrix}. \quad (7)$$

Based on (7), the vehicle model (3) can be further written as

$$\dot{X} = f(X) + BKU, \quad (8)$$

$$\text{with } X = \begin{bmatrix} V_x \\ V_y \\ \Omega_z \end{bmatrix}, B = \frac{B_x}{R_{eff}}, K = \begin{bmatrix} k_{fl} & 0 & 0 & 0 \\ 0 & k_{fr} & 0 & 0 \\ 0 & 0 & k_{rl} & 0 \\ 0 & 0 & 0 & k_{rr} \end{bmatrix}, U =$$

$$\begin{bmatrix} u_{fl} \\ u_{fr} \\ u_{rl} \\ u_{rr} \end{bmatrix}, \text{ and } f(X) = \begin{bmatrix} f_1(X) \\ f_2(X) \\ f_3(X) \end{bmatrix} = \begin{bmatrix} V_y \Omega_z - \frac{C_a}{M} V_x^2 \\ -V_x \Omega_z \\ 0 \end{bmatrix} + B_y F_y -$$

$$\frac{B_x}{R_{eff}} \begin{bmatrix} I \dot{\omega}_{fl} \\ I \dot{\omega}_{fr} \\ I \dot{\omega}_{rl} \\ I \dot{\omega}_{rr} \end{bmatrix}. \text{ The } \dot{\omega}_i \text{ can be estimated in real-time using a}$$

Kalman filter [21].

### B. Problem formulation

When one of the four in-wheel motors/motor drivers has a fault, without accommodating control action, the vehicle may deviate from the expected trajectory as the torque provided by the faulty wheel will be less than expected. In this paper, vehicle longitudinal speed and yaw rate are controlled to follow the references. A fault diagnosis approach and FT controller is designed to maintain the vehicle stability and desired performance when a fault happens. Moreover, it is also desirable that the vehicle controller can automatically relieve the torque demand on the faulty in-wheel motor to avoid further damage. It is assumed that when a fault happens to a motor/driver, the respective control gain will jump to a lower constant value.

Global positioning system (GPS) and inertia measurement unit (IMU) have been proved to be effective in measuring vehicle states [18]. Based on these advanced sensing technologies, the vehicle yaw rate, longitudinal and lateral speeds can be accurately measured. Tire slip ratios, slip angles and the speeds at the wheel centers can also be calculated.

### III. PASSIVE FAULT TOLERANT CONTROL DESIGN

#### A. Straight Line Case

When the vehicle is running in a straight line, the vehicle model can be written as

$$\dot{X} = f(X) + \frac{1}{R_{eff}} \begin{bmatrix} \frac{1}{M} & 0 & 0 \\ 0 & \frac{1}{M} & 0 \\ 0 & 0 & \frac{l_s}{I_z} \end{bmatrix} \begin{bmatrix} 1 & 1 & 1 & 1 \\ 0 & 0 & 0 & 0 \\ -1 & 1 & -1 & 1 \end{bmatrix} KU. \quad (9)$$

The cost function for the four motors can be defined as

$$J = \sum_i w_i u_i^2, \quad (10)$$

$$\text{Subject to } \begin{cases} u_{fr} k_{fr} + u_{rr} k_{rr} = T_r \\ u_{fl} k_{fl} + u_{rl} k_{rl} = T_l \end{cases}$$

with  $w_i$  being the weighting factor for each of the wheels.  $T_r$  and  $T_l$  are the required total motor torques from the right and left sides of the vehicle, respectively. As the four wheels are assumed to be the same, one can make  $w_{rr} = w_{rf} = w_{lr} = w_{lf} = w_0$ . The above cost function can be minimized if the two control signals on the same side of the vehicle are identical, that is

$$\begin{cases} u_l = u_{fl} = u_{rl} \\ u_r = u_{fr} = u_{rr} \end{cases} \quad (11)$$

It can be seen from (9) that the two wheels on the same side of the vehicle have the same effect on the vehicle dynamics. Putting the two wheels on the same side into one subspace, one has

$$\begin{cases} k_{fl} u_{fl} + k_{rl} u_{rl} = u_l k_l \\ k_{fr} u_{fr} + k_{rr} u_{rr} = u_r k_r \end{cases} \quad (12)$$

with

$$\begin{cases} k_l = k_{fl} + k_{rl} \\ k_r = k_{fr} + k_{rr} \end{cases} \quad (13)$$

When a fault happens, the actual value of  $k_l$  or  $k_r$  will be unknown as  $k_i$  is unknown due to the fault. An adaptive controller, which does not need the accurate value of  $k_l$  or  $k_r$ , is proposed to design the passive FTC for stabilizing the faulty vehicle. As the vehicle trajectory is mostly determined by its longitudinal speed and yaw rate, only these two states are controlled to follow the references.

Choose a Lyapunov function candidate as

$$V = \frac{(V_{rx} - V_x)^2 + (\Omega_{rz} - \Omega_z)^2 + (k_l - \hat{k}_l)^2 + (k_r - \hat{k}_r)^2}{2}, \quad (14)$$

where  $V_{rx}$  and  $\Omega_{rz}$  are the longitudinal speed and yaw rate references.  $\hat{k}_l$  and  $\hat{k}_r$  are the estimations of  $k_l$  and  $k_r$ , respectively. The time derivative of the Lyapunov function is

$$\dot{V} = e_{rx} (\dot{V}_{rx} - \dot{V}_x) + e_{\Omega} (\dot{\Omega}_{rz} - \dot{\Omega}_z) - (k_l - \hat{k}_l) \dot{\hat{k}}_l - (k_r - \hat{k}_r) \dot{\hat{k}}_r \quad (15)$$

$$\begin{aligned} &= e_{rx} \left( \dot{V}_{rx} - f_1(X) + \frac{-k_l u_l - k_r u_r}{M R_{eff}} \right) - (k_r - \hat{k}_r) \dot{\hat{k}}_r \\ &\quad + e_{\Omega} \left( \dot{\Omega}_{rz} - f_3(X) + \frac{l_s k_l u_l - l_s k_r u_r}{R_{eff} l_z} \right) - (k_l - \hat{k}_l) \dot{\hat{k}}_l \\ &= e_{rx} (\dot{V}_{rx} - f_1(X)) + e_{\Omega} (\dot{\Omega}_{rz} - f_3(X)) + \hat{k}_l \dot{\hat{k}}_l \\ &\quad + \hat{k}_r \dot{\hat{k}}_r - \left( \frac{e_{rx} k_l u_l}{R_{eff} M} - \frac{e_{\Omega} l_s k_l u_l}{R_{eff} l_z} - k_l \dot{\hat{k}}_l \right) \\ &\quad - \left( \frac{e_{rx} k_r u_r}{R_{eff} M} + \frac{e_{\Omega} l_s k_r u_r}{R_{eff} l_z} - k_r \dot{\hat{k}}_r \right) \end{aligned}$$

where  $e_{rx} = V_{rx} - V_x$ ,  $e_{\Omega} = \Omega_{rz} - \Omega_z$ . By making

$$\begin{cases} \dot{\hat{k}}_l = \left( \frac{e_{rx}}{R_{eff} M} - \frac{l_s e_{\Omega}}{R_{eff} l_z} \right) u_l \\ \dot{\hat{k}}_r = \left( \frac{e_{rx}}{R_{eff} M} + \frac{l_s e_{\Omega}}{R_{eff} l_z} \right) u_r \end{cases}, \quad (16)$$

one can rewrite the derivative of the Lyapunov function as

$$\dot{V} = e_{rx} (\dot{V}_{rx} - f_1(X)) + e_{\Omega} (\dot{\Omega}_{rz} - f_3(X)) \quad (17)$$

$$- \hat{k}_l \left( \frac{e_{rx}}{R_{eff} M} - \frac{l_s e_{\Omega}}{R_{eff} l_z} \right) u_l - \hat{k}_r \left( \frac{e_{rx}}{R_{eff} M} + \frac{l_s e_{\Omega}}{R_{eff} l_z} \right) u_r.$$

If the control law for  $u_l$  and  $u_r$  can be chosen such that

$$\begin{cases} L_1 e_{rx}^2 + e_{rx} (\dot{V}_{rx} - f_1(X)) = \frac{e_{rx}}{R_{eff} M} (\hat{k}_l u_l + \hat{k}_r u_r) \\ L_2 e_{\Omega}^2 + e_{\Omega} (\dot{\Omega}_{rz} - f_3(X)) = \frac{e_{\Omega} l_s}{R_{eff} l_z} (-\hat{k}_l u_l + \hat{k}_r u_r) \end{cases} \quad (18)$$

with  $L_1$  and  $L_2 > 0$ . Then, one has

$$\dot{V} = -L_1 e_{rx}^2 - L_2 e_{\Omega}^2 \leq 0, \quad (19)$$

which means that the actual longitudinal speed and yaw rate can follow their references. Based on (18) we can get the control law as

$$\begin{cases} u_l = \frac{R_{eff} M (L_1 e_{rx} + \dot{V}_{rx} - f_1(X)) - \frac{R_{eff} l_z}{l_s} (L_2 e_{\Omega} + \dot{\Omega}_{rz} - f_3(X))}{2 \hat{k}_l} \\ u_r = \frac{R_{eff} M (L_1 e_{rx} + \dot{V}_{rx} - f_1(X)) + \frac{R_{eff} l_z}{l_s} (L_2 e_{\Omega} + \dot{\Omega}_{rz} - f_3(X))}{2 \hat{k}_r} \end{cases} \quad (20)$$

In order to guarantee the control signals are bounded, a projection method is used to modify the adaption laws [20]. Based on the control gain definition (12), one can see that both  $\hat{k}_l$  and  $\hat{k}_r$  should be bounded as

$$\begin{cases} 0 < \varepsilon \leq \hat{k}_l \leq 2k_{max} \\ 0 < \varepsilon \leq \hat{k}_r \leq 2k_{max} \end{cases}, \quad (21)$$

where  $\varepsilon$  is a small positive constant and  $k_{max}$  is the maximal control gain of a single motor. Note that if only one motor is in fault,  $\varepsilon$  will equal to the single motor minimal control gain  $k_{min}$ . Based on the projection method, the adaption law for  $\hat{k}_l$  in (16) can be modified as:

$$\dot{\hat{k}}_l = \begin{cases} s & \text{if } (0 < \varepsilon < \hat{k}_l < 2k_{max}) \\ & \text{or } (\hat{k}_l = \varepsilon \text{ and } s > 0) \\ & \text{or } (\hat{k}_l = 2k_{max} \text{ and } s < 0) \\ 0 & \text{otherwise} \end{cases}, \quad (22)$$

where  $s$  is defined as  $s = \left( \frac{e_{rx}}{R_{eff} M} - \frac{l_s e_{\Omega}}{R_{eff} l_z} \right) u_l$ . Similarly, the adaption law for  $\hat{k}_r$  can be modified as well.

#### B. Turning Case

When the vehicle is turning, as only the vehicle longitudinal speed and yaw rate are controlled to follow the references, the vehicle model (3) can be written as

$$\begin{bmatrix} \dot{V}_x \\ \dot{\Omega}_z \end{bmatrix} = \begin{bmatrix} f_1(X) \\ f_3(X) \end{bmatrix} + \frac{1}{R_{eff}} \begin{bmatrix} \frac{\cos \sigma}{M} & \frac{\cos \sigma}{M} & \frac{1}{M} & \frac{1}{M} \\ l_f \sin \sigma - l_s \cos \sigma & l_f \sin \sigma + l_s \cos \sigma & -l_s & l_s \\ l_z & l_z & -l_z & l_z \end{bmatrix} KU. \quad (23)$$

With the assumption (11), we can have,

$$\begin{bmatrix} \dot{V}_x \\ \dot{\Omega}_z \end{bmatrix} = \begin{bmatrix} f_1(X) \\ f_3(X) \end{bmatrix} + \frac{1}{R_{eff}} \begin{bmatrix} \frac{1}{M} & 0 \\ 0 & \frac{l_s}{l_z} \end{bmatrix} \begin{bmatrix} k_{lx} & k_{rx} \\ -k_{lz} & k_{rz} \end{bmatrix} \begin{bmatrix} u_l \\ u_r \end{bmatrix} \quad (24)$$

with

$$\begin{cases} k_{lx} = k_{fl} \cos \sigma + k_{rl} \\ k_{rx} = k_{fr} \cos \sigma + k_{rr} \\ k_{lz} = k_{fl} \cos \sigma + k_{rl} - k_{fl} \frac{l_f \sin \sigma}{l_s} \\ k_{rz} = k_{fr} \cos \sigma + k_{rr} + k_{fr} \frac{l_f \sin \sigma}{l_s} \end{cases} \quad (25)$$

Redefine the Lyapunov function candidate as

$$V = \frac{e_{rx}^2 + e_{rz}^2 + (k_{lx} - \hat{k}_{lx})^2 + (k_{rx} - \hat{k}_{rx})^2 + (k_{lz} - \hat{k}_{lz})^2 + (k_{rz} - \hat{k}_{rz})^2}{2} \quad (26)$$

Ignoring the time derivative of the steering angle, the time derivative of the above Lyapunov function can be written as

$$\begin{aligned} \dot{V} &= e_{rx} \left( \dot{V}_{rx} - f_1(X) - \frac{k_{lx} u_l + k_{rx} u_r}{R_{effM}} \right) - (k_{lx} - \hat{k}_{lx}) \dot{\hat{k}}_{lx} \\ &+ e_{\Omega} \left( \dot{\Omega}_{rz} - f_3(X) - \frac{-l_s k_{lz} u_l + l_s k_{rz} u_r}{R_{effLZ}} \right) - \\ &(k_{rx} - \hat{k}_{rx}) \dot{\hat{k}}_{rx} - (k_{lz} - \hat{k}_{lz}) \dot{\hat{k}}_{lz} - (k_{rz} - \hat{k}_{rz}) \dot{\hat{k}}_{rz} \\ &= e_{rx} \left( \dot{V}_{rx} - f_1(X) \right) + e_{\Omega} \left( \dot{\Omega}_{rz} - f_3(X) \right) + \hat{k}_{lx} \dot{\hat{k}}_{lx} \\ &- \left( e_{rx} \frac{k_{lx} u_l}{R_{effM}} + k_{lx} \dot{\hat{k}}_{lx} \right) - \left( e_{rx} \frac{k_{rx} u_r}{R_{effM}} + k_{rx} \dot{\hat{k}}_{rx} \right) \\ &+ \left( e_{\Omega} \frac{l_s k_{lz} u_l}{R_{effLZ}} - k_{lz} \dot{\hat{k}}_{lz} \right) + \left( -e_{\Omega} \frac{l_s k_{rz} u_r}{R_{effLZ}} - k_{rz} \dot{\hat{k}}_{rz} \right) \\ &+ \hat{k}_{rx} \dot{\hat{k}}_{rx} + \hat{k}_{lz} \dot{\hat{k}}_{lz} + \hat{k}_{rz} \dot{\hat{k}}_{rz}. \end{aligned} \quad (27)$$

By making

$$\begin{cases} \dot{\hat{k}}_{lx} = -\frac{e_{rx}}{R_{effM}} u_l \\ \dot{\hat{k}}_{rx} = -\frac{e_{rx}}{R_{effM}} u_r \\ \dot{\hat{k}}_{lz} = \frac{l_s e_{\Omega}}{R_{effLZ}} u_l \\ \dot{\hat{k}}_{rz} = -\frac{l_s e_{\Omega}}{R_{effLZ}} u_r \end{cases}, \quad (28)$$

one can write the derivative of the Lyapunov function as

$$\begin{aligned} \dot{V} &= e_{rx} \left( \dot{V}_{rx} - f_1(X) \right) + e_{\Omega} \left( \dot{\Omega}_{rz} - f_3(X) \right) - \frac{e_{rx} u_l \hat{k}_{lx}}{R_{effM}} \\ &- \frac{e_{rx} u_r \hat{k}_{rx}}{R_{effM}} + \frac{l_s e_{\Omega} u_l \hat{k}_{lz}}{R_{effLZ}} - \frac{l_s e_{\Omega} u_r \hat{k}_{rz}}{R_{effLZ}}. \end{aligned} \quad (29)$$

The following equations

$$\begin{cases} L_1 e_{rx}^2 + e_{rx} \left( \dot{V}_{rx} - f_1(X) \right) = \frac{e_{rx}}{R_{effM}} (\hat{k}_{lx} u_l + \hat{k}_{rx} u_r) \\ L_2 e_{\Omega}^2 + e_{\Omega} \left( \dot{\Omega}_{rz} - f_3(X) \right) = \frac{l_s e_{\Omega}}{R_{effLZ}} (-\hat{k}_{lz} u_l + \hat{k}_{rz} u_r) \end{cases} \quad (30)$$

can make (19) holds. Thus, the control law for the turning case can be written as

$$\begin{cases} u_l = \frac{R_{eff} \left( M \hat{k}_{lz} (L_1 e_{rx} + (\dot{V}_{rx} - f_1(X))) - \frac{l_s}{R_{eff}} \hat{k}_{lx} (L_2 e_{\Omega} + (\dot{\Omega}_{rz} - f_3(X))) \right)}{\hat{k}_{lx} \hat{k}_{rz} + \hat{k}_{rx} \hat{k}_{lz}} \\ u_r = \frac{R_{eff} \left( M \hat{k}_{lz} (L_1 e_{rx} + (\dot{V}_{rx} - f_1(X))) + \frac{l_s}{R_{eff}} \hat{k}_{lx} (L_2 e_{\Omega} + (\dot{\Omega}_{rz} - f_3(X))) \right)}{\hat{k}_{lx} \hat{k}_{rz} + \hat{k}_{rx} \hat{k}_{lz}} \end{cases} \quad (31)$$

Based on the definition of  $k_j$  in (25), with  $j = \{lx, rx, lz, rz\}$  stand for a specific control gain, the  $\hat{k}_j$  should be bounded as

$$0 < \varepsilon \leq \hat{k}_j \leq \left( \sqrt{\frac{l_s^2 + l_f^2}{l_s}} + 1 \right) k_{max}. \quad (32)$$

Similar to the adaption law modification as (22) shows, the adaption law for  $\hat{k}_j$  shown in (28) can also be modified with the projection method to guarantee the control signals are bounded. Note that the controller design for the vehicle running in a straight line is a special case of vehicle in turning. Thus, this controller can also be used in the straight

line driving situations. Simulation results also echo this.

#### IV. ACTIVE FAULT DIAGNOSIS DESIGN AND CONTROL EFFORT REDISTRIBUTION

The passive FT controller designed in the previous section is not an ideal one as the torque demand on the faulty wheel is not specifically reduced. It is better to actively adjust the weighting factor of the faulty motor in the cost function to discourage use of the faulty motor. It can be seen from (9) or (24) that the two wheels on the same side have the same effect on the vehicle speed/yaw rate. So, an active fault diagnosis method is proposed in this section to explicitly locate the faulty wheel and estimate its control gain to better allocate the control efforts.

Suppose that the passive FT controller for the healthy vehicle can give a control signal  $U_0$  which can maintain the vehicle in the desired trajectory. For the vehicle running in a straight line, one has the following holds

$$\begin{cases} u_l (k_{fl} + k_{rl}) = u_{0l} (k_{0fl} + k_{0rl}) \\ u_r (k_{fr} + k_{rr}) = u_{0r} (k_{0fr} + k_{0rr}) \end{cases} \quad (33)$$

As  $k_i \neq k_{0i}$  means a fault happens to a wheel, one has

$$\begin{cases} u_j = u_{0j} \text{ no fault happens} \\ u_j \neq u_{0j} \text{ a fault happens} \end{cases} \quad (34)$$

with  $j$  indicating the left or right side. For the two wheels on the faulty side, the two motor control gains  $k_1$  and  $k_2$  satisfy

$$k_1 + k_2 = \frac{(k_{01} + k_{02}) u_{0f}}{u_f}, \quad (35)$$

where  $u_f$  is the control signal for the faulty side motors after the fault happens. It can be seen that there are two unknown parameters,  $k_1$  and  $k_2$ , in the above equation, which means the actual control gain of the faulty wheel cannot be solved from (35) alone. So another equation should be used to calculate the two control gains on the faulty side. As the motor control gain can be virtually changed by multiplying a positive value,  $\alpha$ , to the control signal. After this additional fault is introduced, one has

$$\alpha k_1 + k_2 = \frac{(k_{01} + k_{02}) u_{0f\_new}}{u_{f\_new}}, \quad (36)$$

where  $u_{f\_new}$  is the faulty side motor control signal after the introduction of this virtual fault. Based on (35) and (36), one can solve for the two control gains  $k_1$  and  $k_2$  for the two motors on the faulty side, and the estimated faulty wheel control gain will be different from the nominal value. Note that the FT controller designed in the previous section can still make the vehicle follow the references even this additional virtual fault is introduced. Also this virtual fault should be introduced only after all the vehicle states have reached the references by the passive FT controller.

Considering the cost function for the two wheels on the faulty side

$$J = w_0 u_h^2 + w_f u_f^2, \quad (37)$$

$$\text{Subject to } u_h k_0 + u_f k_f = T_d,$$

where  $T_d$  is the desired motor total torque from this side.  $u_h$  and  $u_f$  are the healthy motor and the faulty motor control gains on this side,  $w_h$  and  $w_f$  are the corresponding weighting factors for the two motors. By Lagrange multiplier

method, one can see the cost function can be minimized if  $u_h$  and  $u_f$  satisfy

$$\frac{u_h}{u_f} = \frac{w_f k_0}{w_0 k_f}. \quad (38)$$

One possible weighting definition for the faulty wheel can be

$$w_f = \frac{k_0 w_0}{k_f}. \quad (39)$$

Based on the above weighting definition,  $u_h$  and  $u_f$  satisfy

$$\frac{u_h}{u_f} = \frac{k_0^2}{k_f^2}. \quad (40)$$

It can be seen that the weighting factors do not change when there is no fault. However, if there is a fault, the faulty wheel control gain decreases and  $w_f$  will increase. If the loss of control gain is large, the associated component will be more heavily weighted. And  $w_f \rightarrow \infty$  if the actual control gain of the faulty wheel goes to 0, which means that the faulty wheel will not be used. The estimated faulty wheel control gain will be used as  $k_f$  in (40).

For the turning case, (33) can be rewritten as,

$$\begin{cases} u_l(\cos \sigma k_{fl} + k_{rl}) = u_{0l}(\cos \sigma k_{0fl} + k_{0rl}) \\ u_r(\cos \sigma k_{fr} + k_{rr}) = u_{0r}(\cos \sigma k_{0fr} + k_{0rr}) \end{cases} \quad (41)$$

In a similar way, the active diagnosis approach for the turning vehicle can be designed.

## V. SIMULATION STUDIES

Two simulation cases based on a high-fidelity full-vehicle model constructed in CarSim were conducted. Vehicle parameters were taken from an actual prototyping 4WID electric vehicle [22]. A driver model was used to generate the reference signals.

### A. J-turn simulation

In this simulation, the nominal control gain of each motor was set to 30, and a fault, reduced control gain, was introduced to the rear-left motor after 2s. At 2.25s the FT controller had stabilized the vehicle, and the virtual fault was introduced to the front-left motor by multiplying the control signal to this motor with  $\alpha = 0.5$ . The faulty wheel control gain estimation is shown in Figure 2. It can be seen that the estimated control gain of the faulty wheel is very close to the actual value. Based on the estimated fault wheel control gain, the weighting factor for the fault wheel in the cost function was readjusted to better allocate the control efforts.

The torque values provided by all the motors are shown in Figure 3. It can be seen that the two wheels on the healthy side always provided the same torque no matter whether there was a fault or not on the other side. After 2s, the healthy motor on the faulty side increased the torque, as the passive FT controller increased more control effort to the faulty side to compensate the tracking error caused by the faulty motor. At 2.25s, the two motors on the faulty side started providing the same torque, this is because the same control signals were still sent to the two motors and the control gains of these two motors became the same due to the virtual fault introduced to the healthy motor. At 2.6s, the active diagnosis period finished, and the healthy motor on the left side began to provide most of the torque required for this side as the control

efforts were redistributed according to the change of the weight factor in the cost function.

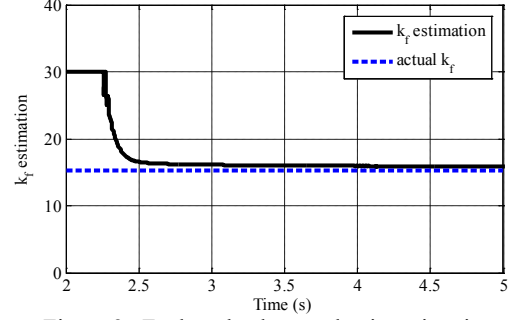


Figure 2. Faulty wheel control gain estimation.

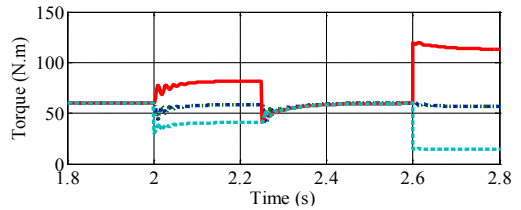
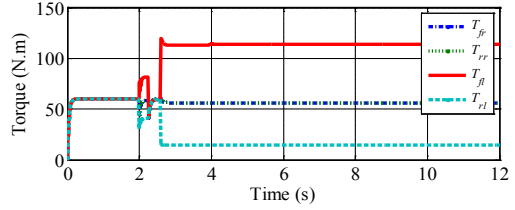


Figure 3. Motor torques in the J-turn simulation.

To better show the effectiveness of the proposed controller, the performance of an uncontrolled vehicle with the same fault was also studied. Figure 4 shows the longitudinal velocity and yaw rate under the proposed fault diagnosis and FT controller. It can be seen from Figure 4 and Figure 5 that the controlled vehicle can follow the reference velocity and yaw rate well, while the uncontrolled vehicle failed to follow the references as the faulty wheel failed to provide the required torque.

### B. Single lane change

In this simulation, the desired vehicle speed was accelerated from 60km/h to 86km/h in 12 seconds. A counter-clockwise turn was introduced. At 3s, a fault was added to the rear-left motor which made the control gain decrease to 30% of its nominal value. Simulation results are shown in Figures 6 and 7. It can be seen again that the controlled vehicle can follow the expected trajectory, while the vehicle without control deviated from the reference as soon as the fault was introduced.

## VI. CONCLUSIONS

A passive FT controller was designed to maintain the vehicle stability and desired performance when a fault happens. An active fault diagnosis approach was proposed to isolate and evaluate the fault under the designed passive FTC. Based on an active in-wheel motor/motor driver fault detection mechanism, the control efforts among the wheels can be redistributed to minimize the cost function considering the fault. Simulations using a high-fidelity CarSim<sup>®</sup> full-vehicle model show the effectiveness of the proposed

fault diagnosis and fault-tolerant control approaches.

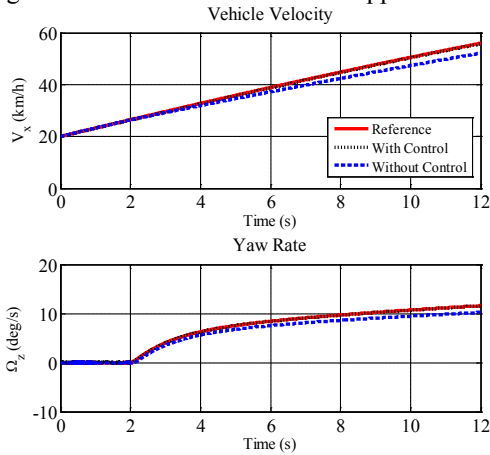


Figure 4. Longitudinal velocities and yaw rates in the J-turn simulation.

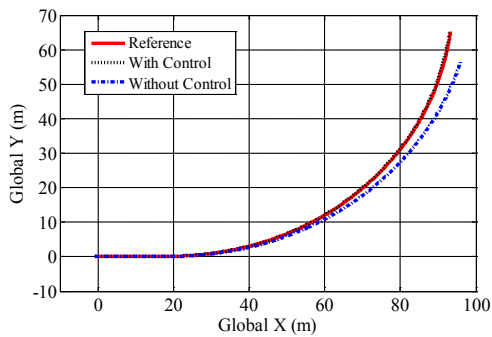


Figure 5. Vehicle trajectories in the J-turn simulation.

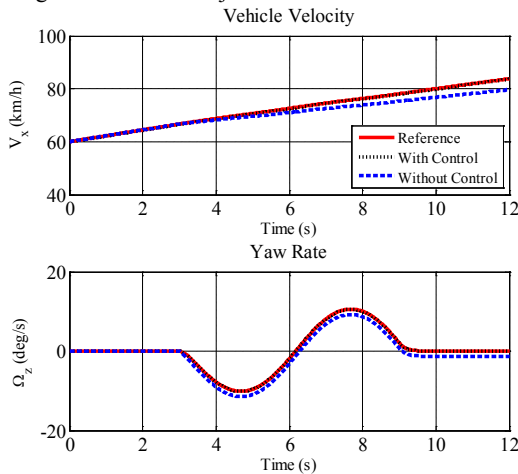


Figure 6. Longitudinal velocities and yaw rates in single lane change.

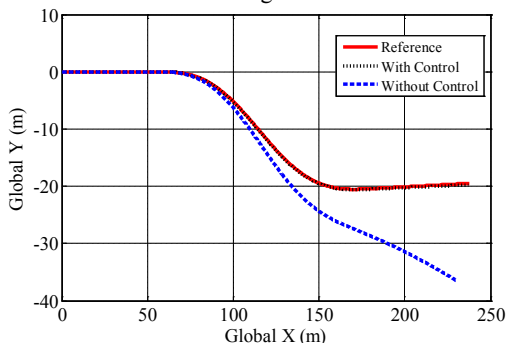


Figure 7. Vehicle trajectories in single lane change.

## REFERENCES

- [1] Chan, C. C., 2002. "The state of the art of electric and hybrid vehicles," Proc. IEEE, 90, pp. 247.
- [2] Wang, J. and Longoria, R.G. "Coordinated and Reconfigurable Vehicle Dynamics Control," IEEE Transactions on Control Systems Technology, Vol. 17, No. 3, pp. 723 – 732, May 2009.
- [3] Shino, M. and Nagai, M., 2003. "Independent wheel torque control of small-scale electric vehicle for handling and stability improvement," JSAE Review, 24(4), October, pp.449-456, 2003.
- [4] R. Wang and J Wang, "In-Wheel Motor Fault Diagnosis for Electric Ground Vehicles," Proceedings of the 2010 ASME Dynamic Systems and Control Conference, 2010.
- [5] R. Wang and J. Wang, "Fault-Tolerant Control of Electric Ground Vehicles with Independently-Actuated Wheels," Proceedings of the 2010 ASME Dynamic Systems and Control Conference, 2010.
- [6] Liang, W., Yu, H., McGee, R., M. Kuang, and J. Medanic, 2009. "Vehicle Pure Yaw Moment control using differential tire slip," American Control Conference, 2009. 10-12 June, pp. 3331 – 3336.
- [7] S. Anwar and L. Chen,(2007), An Analytical Redundancy-Based Fault Detection and Isolation Algorithm for a Road-Wheel Control Subsystem in a Steer-By-Wire System, IEEE Trans on Vehicular Technology, 56(5), 2007.
- [8] Jayabalan, R., and Fahimi, B. "Monitoring and Fault Diagnosis of Multiconverter Systems in Hybrid Electric Vehicles," IEEE Trans. on Vehicular Technology, 55(5), pp.1475 – 1484, 2006.
- [9] R. Isermann, R. Schwartz, and S. Stolz, "Fault-tolerant drive-by-wire systems," IEEE Control Syst. Mag., vol. 27, no. 5, pp. 64–81, Oct. 2002.
- [10] Wu, J.D., Chuang, C.Q., 2005. "Fault diagnosis of internal combustion engines using visual dot patterns of acoustic and vibration signals," NDT & E International, 38(8), December, pp. 605-614.
- [11] Nyberg, M. and Stutte, T. 2004. "Model based diagnosis of the air path of an automotive diesel engine," Control Engineering Practice, 12(5), May, pp. 513-525.
- [12] N. Meskin and K. Khorasani,(2007), "Fault Detection and Isolation of Actuator Faults in Overactuated Systems", Proceedings of the 2007 American Control Conference, July 11-13, 2007,pp 2527-2532.
- [13] H. Yang, V. Cocquempot, and B. Jiang. (2010). "Optimal Fault-Tolerant Path-Tracking Control for 4WS4WD Electric Vehicles", IEEE Trans.on Inte. Tran. systems, 11(1), pp 237-243.
- [14] H. Yang, V. Cocquempot, and B. Jiang. (2010). "Hybrid Fault Tolerant Tracking Control Design for Electric Vehicles", 16th Mediterranean Conference on Control and Automation Congress Centre, Ajaccio, France, June 25-27, 2008.
- [15] O. Wallmark, L. Harnefors, and O. Carlson. (2007). "Control Algorithms for a Fault-Tolerant PMSM Drive" IEEE Trans on Industrial Electronics, 54(4), August 2007.
- [16] Jo Yung Wong, Theory of Ground Vehicles, 3rd Edition. New York: Wiley, 2001.
- [17] Muenchhof, M., Beck, M. and Isermann, M. (2009). "Fault-tolerant actuators and drives—Structures, fault detection principles and applications", Annual Reviews in Control, 33, pp. 136–148.
- [18] S. Di Cairano and H.E. Tseng. "Driver-assist steering by active front steering and differential braking: design, implementation and experimental evaluation of a switched model predictive control approach," Proceedings of the 49th IEEE Conference on Decision and Control, pp. 2886 – 2891, Dec. 2010.
- [19] I. Hwang, S. Kim, Y. Kim, and C. E. Seah. (2010). "A Survey of Fault Detection, Isolation, and Reconfiguration Methods", IEEE Trans on Control Systems Technology, 18(3), pp 636-653.
- [20] G. Tao, Adaptive Control Design and Analysis. New York: Wiley, 2003.
- [21] J.D. Han, Y.Q. He, and W.L. Xu. "Angular acceleration estimation and feedback control: An experimental investigation", Mechatronics 17 (2007) 524–532.
- [22] R. Wang, Y. Chen, D. Feng, X. Huang, and J. Wang, "Development and Performance Characterization of an Electric Ground Vehicle with Independently Actuated In Wheel Motors," Journal of Power Sources, Vol. 196, No 8, pp. 3962-3971, 2011.
- [23] Chen, Y. and Wang, J., "Adaptive Vehicle Speed Control with Input Injections for Longitudinal Motion Independent Road Frictional Condition Estimation," IEEE Transactions on Vehicular Technology, Vol. 60, No. 3, pp. 839 - 848, 2011.